Journal of Veterinary Internal Medicine

Journal of Veterinary Internal Medicine Open Access
ACVIM American College of Veterinary Internal Medicine

STANDARD ARTICLE OPEN ACCESS
Small Animal Internal Medicine Neurology

Evolution of Brain Magnetic Resonance Imaging Lesions in Dogs Treated for Meningoencephalomyelitis of Unknown Origin Between Initial Diagnosis and Relapse

Carole Soulé[1] | Laurent Blond[1] | Robin Cavalerie[2] | Stéphanie Piazza[2] | Clément Baudin-Tréhiou[1]

[1]Department of Diagnostic Imaging, Centre Hospitalier Vétérinaire Languedocia, Montpellier, France | [2]Department of Neurology, Centre Hospitalier Vétérinaire Languedocia, Montpellier, France

Correspondence: Carole Soulé (carole.soule9@gmail.com)

Received: 6 September 2024 | **Revised:** 14 March 2025 | **Accepted:** 31 March 2025

Funding: The authors received no specific funding for this work.

Keywords: canine | control | follow-up | granulomatous meningoencephalitis | meningoencephalitis of unknown etiology | MRI | necrotizing encephalitis | necrotizing leukoencephalitis | necrotizing meningoencephalomyelitis

ABSTRACT

Background: The response of meningoencephalitis of unknown origin (MUO) in dogs to immunosuppressive treatment is unpredictable, and relapses frequently occur.

Objectives: Our aim was to describe the evolution of brain magnetic resonance imaging (MRI) lesions in dogs treated for MUO from diagnosis to relapse and to define the diagnostic and clinical value of repeat MRI at relapse.

Animals: Eighteen dogs treated for MUO that experienced relapse and underwent MRI both at disease onset and relapse.

Methods: Retrospective, descriptive, longitudinal, case series study. Dogs were identified from medical records between 2015 and 2024. The MR images were reviewed by radiologists for lesion number, location, size, pre- and post-contrast signal aspect, meningeal enhancement, mass effect, perilesional edema, and evidence of intracranial hypertension.

Results: Median interval between MRIs was 259 days (range, 31–876 days). In dogs with relapse delay < 157 days, lesion number tended to decrease. Residual lesions tended to enlarge and exhibit contrast enhancement and perilesional edema (suggesting an active pathologic process), but without development of new lesions. After 233 days, all dogs had developed new lesions. Half exhibited enlarged active residual lesions, whereas the others showed either remission or smaller inactive lesions.

Conclusions: Before a clinical relapse at approximately 6 months, remission of the initial pathologic process and development of new lesions appear unlikely. Beyond this period, new lesions may occur with or without remission of the initial pathologic process, and repeat MRI is of high diagnostic and clinical value in detecting new lesions and characterizing the underlying pathologic process.

1 | Introduction

In dogs, the term meningoencephalitis of unknown origin (MUO) refers to two types of idiopathic, non-infectious, inflammatory central nervous system (CNS) diseases, granulomatous meningoencephalomyelitis (GME), and necrotizing encephalitis (NE), as well as two NE subtypes, necrotizing meningoencephalomyelitis (NME) and necrotizing leukoencephalitis (NLE),

Abbreviations: CSF, cerebrospinal fluid; DICOM, digital imaging and communications in medicine; GME, granulomatous meningoencephalomyelitis; MRI, magnetic resonance imaging; MUE, meningoencephalitis of unknown etiology; MUO, meningoencephalitis of unknown origin; NE, necrotizing encephalitis; NLE, necrotizing leukoencephalitis; NME, necrotizing meningoencephalomyelitis.

when definitive histopathologic diagnosis is unavailable [1–4]. Differences in lesion severity and topography between NME and NLE may reflect breed-specific immune response variability [5]. Small breeds (e.g., Pug, Maltese, Chihuahua, Pekingese, French Bulldog, Shi Tzu, Lhasa Apso, Yorkshire Terrier) and young adults are overrepresented, with recent studies reporting no significant female-to-male ratio differences [1, 2, 4, 6, 7]. Presumptive diagnosis relies on multiple factors, including signalment, history, clinical abnormalities, cerebrospinal fluid (CSF) analysis, negative tests for infectious diseases, and magnetic resonance imaging (MRI) [7]. Pleocytosis in CSF is a diagnostic criterion, but CSF cytology may be normal in 3%–57% of cases [1, 2, 4, 8, 9]. Histopathologic confirmation is rarely achieved antemortem because of cost, limited availability, and the invasiveness of brain biopsy, despite being relatively safe [10–13]. The efficacy of immunosuppressive treatment supports an immune-mediated etiology, but underlying mechanisms remain unclear [1, 14, 15]. Research on diagnostic biomarkers for MUO and its subtypes is promising but remains in early stages of development [16]. Magnetic resonance imaging can play a role in differentiating MUO subtypes. Common MUO lesion features include irregular, ill-defined margins, T2-weighted (T2W) hyperintensity, and T1-weighted (T1W) hypo- to isointensity, with variable lesional contrast enhancement, perilesional edema, and ventriculomegaly. Necrotizing encephalitis may feature lesions with T2W fluid-attenuated inversion recovery (T2W-FLAIR) signal suppression because of necrosis, and NLE may feature white matter-restricted lesions lacking meningeal enhancement or mass effect [1, 3, 4, 7, 17–21]. Lesions of GME may be focal or multifocal, affecting the forebrain, brainstem, cerebellum, or optic nerves, whereas NE lesions are typically multifocal, with NME lesions primarily involving the forebrain and NLE lesions affecting both the forebrain and brainstem [1, 3, 4, 7, 17–21]. Histopathologic features of MUO subtypes are well-documented [15, 22], and MRI abnormalities generally correlate with histopathologic findings [18]. However, MRI alone cannot reliably distinguish histopathologic patterns and remains imperfect, because up to 40% of cases have undetected lesions, and 7%–26% of affected dogs appear normal, even using high-field MRI scanners [1, 2, 4, 23]. Follow-up typically depends on clinical response and may include repeated CSF analysis, MRI, or both [4]. Prognosis is variable and unpredictable. Granulomatous meningoencephalitis carries a guarded prognosis, whereas NE is associated with a poor outcome [7]. Relapse occurs in up to 65% of cases, with a median delay of 210 days (7 months) [24, 25]. To our knowledge, no study has described the MRI evolution of MUO brain lesions between diagnosis and relapse in dogs. We aimed to document lesion evolution using low-field MRI from diagnosis to relapse and evaluate the diagnostic and clinical value of repeat MRI at relapse.

2 | Materials and Methods

2.1 | Selection of Cases

This retrospective, descriptive, longitudinal case series study utilized medical records of client-owned dogs admitted to our institution between May 2015 and March 2024. The inclusion criteria were: (1) a presumptive MUO diagnosis, including brain MRI, (2) administration of immunosuppressive treatment with subsequent improvement or resolution of clinical signs, (3) relapse, and (4) a second brain MRI. Physical and neurological examinations, clinical neurolocalization, presumptive MUO diagnosis, treatment response, and relapse were assessed by an European College of Veterinary Neurology (ECVN) board-certified veterinary neurologist (S.P.). The guidelines for presumptive diagnosis included: (1) dogs > 6 months, (2) intra-axial T2-weighted (T2W) hyperintensities (multiple, single, or diffuse) on magnetic resonance (MR) images, (3) monocytic or lymphocytic pleocytosis on cerebrospinal fluid (CSF) analysis, and (4) exclusion of infectious agents [2, 4]. Dogs < 6 months, those with missing initial or relapse imaging, or those lacking initial CSF analysis were excluded. Imaging studies were reviewed and approved for inclusion by an American College of Veterinary Radiology (ACVR; L.B.) or European College of Veterinary Diagnostic Imaging (ECVDI; C.B.T.) board-certified veterinary radiologist.

2.2 | Data Collection and Analysis

Cases meeting the aforementioned criteria presented to our institution between May 2015 and March 2024 were identified, and data were retrieved from electronic medical records by a diagnostic imaging resident (C.S.).

2.2.1 | Initial Clinical Data

Initial clinical data collected included weight, breed, sex, neuter status, age at initial MRI, onset of clinical signs, clinical neurolocalization, and concurrent treatment at admission.

2.2.2 | Initial MRI Data Acquisition

All dogs underwent initial MRI under general anesthesia using a standardized protocol at our institution. Imaging was performed using a 0.25 Tesla MRI scanner (ESAOTE Vet-MR Grande 0.25T, Genova, Italy) and an elliptical receiving coil (dual phased-array) adapted to the patient's head size. Dogs were positioned in ventral recumbency. A standardized protocol was used, including sagittal and transverse 2-dimensional (2D) fast spin echo (FSE) T2-weighted (T2W), transverse 2D FSE T2W fluid-attenuated inversion recovery (T2W-FLAIR), dorsal 3-dimensional hybrid contrast enhancement (3D HYCE), 3D steady-state (SS) gradient recalled echo (GRE) T2W), pre- and post-contrast transverse spin echo (SE) T1-weighted (T1W), and post-contrast dorsal 3D GRE T1W (3D SS T1 or 3D turbo T1) images. Post-contrast images were obtained after iv injection of 0.1 mmol/kg gadopentate dimeglumine (0.5 mmol/mL) without a pressure injector. Acquisition delays after contrast media administration were approximately 1 min for post-contrast dorsal 3D SS T1 or 3D Turbo T1 images and 7 min for transverse SE T1W images.

2.2.3 | Initial Diagnosis, Treatment, and Outcome

After the initial MRI, CSF was collected from all anesthetized dogs. Puncture site (cerebellomedullary cistern or lumbar subarachnoid space), cytological analysis, protein concentration,

and methods to exclude infectious agents were recorded. All dogs received an immunosuppressive protocol combining prednisolone with either cytosine arabinoside or cyclosporine. Initial doses were 2 mg/kg/day PO for prednisolone, 200 mg/m [2] administered by continuous infusion over 12–24 h or 400 mg/m [2] via four SC injections q12–24 h every 3–4 weeks for six cycles for cytosine arabinoside, and 5 mg/kg/day PO for cyclosporine, with dose tapering and duration adjusted based on clinical response.

2.2.4 | Control MRI Data Acquisition (Between Initial and Relapse MRI)

Some dogs underwent control MRI, CSF analysis, or both months after initiating immunosuppressive treatment to assess lesion evolution, determine relapse risk, and adjust medication. Clinical neurolocalization and concurrent treatments at admission were recorded. All control MRIs were performed at our institution under the same conditions as the initial MRI, following a standardized protocol that included sagittal and transverse 2D FSE T2W, transverse 2D FSE T2W-FLAIR, and pre- and post-contrast transverse SE T1W images.

2.2.5 | Relapse Diagnosis

Clinical neurolocalization and concurrent treatments at admission were recorded. All dogs underwent MRI at relapse at our institution under the same conditions as the control examination. Relapse diagnosis was based on physical and neurological examination, CSF analysis, diagnostic imaging, or some combination of these.

2.2.6 | Image Analysis Protocol and Grading Criteria

The MR images were reviewed independently, and in cases of discrepancy, collaboratively to reach a consensus by an ACVR (L.B.) or ECVDI (C.B.T.) board-certified veterinary radiologist and a diagnostic imaging resident (C.S.), using workstations equipped with a 21.5-inch. Retina 4 K display (Apple, Cupertino, California) and a digital imaging and communications in medicine (DICOM) viewer (Osirix, Bernex, Switzerland). Observers were aware of the MUO diagnosis before interpretation.

Initial, control, and relapse MR images were analyzed for: (1) lesion number, (2) localization, (3) size (maximum diameter), (4) pre-contrast signal aspect (including intensity, uniformity, and delineation on T2W and pre-contrast T1W images, and signal suppression on T2W-FLAIR images), (5) lesional contrast enhancement characteristics (degree, uniformity, and delineation on post-contrast T1W), (6) degree of meningeal enhancement, (7) mass effect, (8) perilesional edema, and (9) evidence of intracranial hypertension.

For localization, the brain was divided into forebrain (telencephalon, diencephalon), midbrain, and hindbrain (pons, medulla oblongata, cerebellum). The telencephalon was further subdivided into the frontal, parietal, temporal, piriform, and occipital lobes, and the diencephalon into the thalamic region and optic chiasm.

Lesion signal intensity was compared with that of surrounding brain tissue. Lesional contrast enhancement, categorized as low, moderate, or strong on postcontrast T1W images, was subjectively compared with pre-contrast T1W images.

Perilesional edema was defined as T2W and T2W-FLAIR hyperintensity and T1W hypo- to isointensity without contrast enhancement in the tissue adjacent to the lesion, with a possible associated mass effect [7, 26]. Mass effect was described as compression of brain structures, potentially resulting in contralateral midline shift, ventricular compression or obstruction, and transtentorial or foramen magnum cerebellar herniation or both [7, 26]. Brain herniation was assessed based on morphometric criteria [27]. Intracranial hypertension was presumed to be present based on a combination of the MRI features identified in a previous study (brain herniation, mass effect, and optic nerve sheath diameter) [28], and sulcal attenuation. Incomplete ossification of the supraoccipital bone and Chiari-like malformation can contribute to foramen magnum cerebellar herniation [29–31]. When these congenital anomalies were present, differentiation was made between malformative herniation and hypertensive herniation secondary to MUO. Chiari-like malformation was identified based on MRI criteria previously described [31].

2.2.7 | Statistical Analysis

Data were entered into spreadsheet software (Microsoft Excel for Mac, version 16.84, Redmond, Washington), and descriptive statistical analyses were conducted by a diagnostic imaging resident (C.S.) using statistical software (XLSTAT, Lumivero, Denver, Colorado). The normality of quantitative data was assessed using the Shapiro–Wilk test. For normally distributed data, results were reported as the mean, whereas non-normally distributed data were presented as the median.

3 | Results

3.1 | Initial Clinical Findings (Tables 1 and 2)

Eighteen dogs met the inclusion criteria. The majority were female, young adults of small breed. The female-to-male ratio was 2:1, with a mean age of 3.5 years (range, 7 months-9.4 years), and no dog weighed > 12.5 kg (median, 3.3 kg). The most common breeds were Chihuahua (7/18, 39%), French Bulldog (4/18, 22%), and Yorkshire Terrier (4/18, 22%), accounting for 83% (15/18) of cases. Clinical signs were predominantly chronic (12/18, 66%) or subacute (5/18, 28%), with a median duration of 27.5 days before admission. Findings were consistent with reported epidemiologic data, except for the predominance of female dogs (12/18, 67%). At the time of the initial MRI, 9/18 (50%) dogs were receiving ongoing immunosuppressive or anti-inflammatory treatment.

3.2 | Initial MRI Findings (Tables 2–4 and Figures 1–3)

Lesions number ranged from 1 to 5 per dog, with a median of 3.5. Multifocal lesions were common (16/18, 89%) and frequently bilateral (13/16, 81%). All dogs with multifocal lesions (16/16,

TABLE 1 | Descriptive statistics for signalment.

	n **= 18**
Mean age (min/max) (IQR) in year	3.4 (0.6/9.4) (3.5)
Median bodyweight (min/max) (IQR) in kg	3.3 (1.4/12.5) (5.7)
Sex Female-to-male ratio	2:1
Neutered status	
Intact	11/18 (61%)
Neutered	7/18 (39%)
Breed	
PB (*n* = 6) and CB (*n* = 1) Chihuahuas	7/18 (39%)
PB French Bulldogs	4/18 (22%)
PB Yorkshire Terriers	4/18 (22%)
Other breeds (PB Maltese dog, PB Pomeranian and PB Shih Tzu)	3/18 (17%)

Abbreviations: CB, crossbreed; PB, purebred.

100%) had at least one forebrain lesion, and 10/16 (62.5%) had forebrain lesions only. All dogs with focal lesions (2/2, 100%) had hindbrain involvement. No midbrain lesions were observed. Forebrain involvement was detected in 16/18 (89%) dogs. Diencephalic lesions were present in 10/18 (56%) dogs, primarily localized to the thalamus (9/10, 90%). Telencephalic lesions were observed in 15/18 (83%) dogs, most frequently in the frontal lobes (11/15, 73%), followed by the parietal (9/15, 60%), occipital (7/15, 47%), and temporal lobes (6/15, 40%). Hindbrain lesions were present in 8/18 (44%) dogs, all (8/8, 100%) affecting the pons, with 5/8 (63%) limited to a single pontine localization. All dogs (18/18, 100%) exhibited irregular, ill-defined T2W hyperintense and T1W iso- to hypointense lesions. Lesional contrast enhancement was common (15/18, 83%). Perilesional edema (13/18, 72%) and mass effect (11/18, 61%) were frequent, whereas T2W-FLAIR suppression (5/18, 28%) and meningeal enhancement (4/18, 22%) were less common. Suspected intracranial hypertension was identified in 9/18 (50%) dogs. Neurolocalization on MRI corresponded to clinical neurolocalization in all cases (18/18, 100%), suggesting that lesions were likely responsible for clinical signs. The lesion distribution, localization, and lesional MRI features and associated findings were consistent with those expected in MUO.

TABLE 2 | Descriptive statistics for initial, control, and relapse clinical findings and ongoing immunosuppressive (IS) treatment and anti-inflammatory (AI) medication.

	Initial diagnosis	**Control**	**Relapse**	**Evolution between initial diagnosis and relapse**
	n **= 18**	***n*** **= 8**	***n*** **= 18**	
Onset of clinical signs				
Acute (< 3 days)	1/18 (6%)	n/a	9/18 (50%)	+44 pp
Subacute (3–15 days)	5/18 (28%)	n/a	5/18 (28%)	0 pp
Chronic (> 15 days)	12/18 (66%)	n/a	3/18 (17%)	−50 pp
No clinical signs	0/18 (0%)	n/a	2/18 (11%)	+11 pp
Clinical neurolocalization				
Multifocal	10/18 (56%)	2/8 (25%)	9/18 (50%)	−6 pp
Prosencephalon	5/18 (28%)	0/8 (0%)	4/18 (22%)	−6 pp
Brainstem/Vestibular system	3/18 (16%)	0/8 (0%)	2/18 (11%)	−5 pp
No neurological signs	0/18 (0%)	6/8 (75%)	3/18 (17%)	+17 pp
Ongoing IS or AI treatment at admission				
Present	9/18 (50%)	8/8 (100%)	13/18 (72%)	+22 pp
Prednisolone	6/18 (33%)	8/8 (100%)	13/18 (72%)	+39 pp
Median dose	1.14 mg/kg/d	0.33 mg/kg/d	0.58 mg/kg/d	
(min–max)	(0.24–2.4)	(0,125–0.57)	(0.04–2.27)	
Cytosine arabinoside	1/18 (6%)	7/8 (88%)	11/18 (61%)	+55 pp
Cyclosporine	0/18 (0%)	1/8 (13%)	0% (0%)	0 pp
Dose	/	5 mg/kg/d	/	
NSAID and other AI drugs	3/18 (17%)	0/8 (0%)	0/18 (0%)	−17 pp
Absent	9/18 (50%)	0/8 (0%)	5/18 (28%)	−22 pp

Abbreviations: AI, anti-inflammatory; d, day; IS, immunosuppressive; NSAID, non-steroidal anti-inflammatory drug; pp, percentage point.

3.3 | Treatment After MRI Imaging and Effect on Initial Clinical Signs

All dogs received immunosuppressive treatment. Among them, 17/18 (94%) were treated with prednisolone and cytosine arabinoside, whereas 1/18 (6%) received cyclosporine and prednisolone. After treatment initiation, 10/18 (56%) achieved complete resolution of clinical signs, whereas 8/18 (44%) experienced marked improvement.

3.4 | Control MRI Findings (Between Initial and Relapse MRI) (Tables 2, 5–6 and Figure 3)

Control MRI was performed during immunosuppressive treatment in 8/18 (44%) dogs, with a median delay of 147 days (range,105–253). At the time of control MRI, 6/8 (75%) dogs exhibited complete clinical resolution, whereas 2/8 (25%) showed marked improvement. The median number of lesions decreased by 71% from 3.5 to 1 per dog, with no new lesions detected. In all dogs with residual lesions (6/6, 100%), these lesions had decreased in size but retained their irregular, ill-defined T2W hyperintense and T1W iso- to hypointense appearance. All lesions with initial T2W-FLAIR signal suppression (3/3, 100%) retained this feature. Lesional contrast enhancement (7/7, 100%), perilesional edema (5/5, 100%), mass effect (4/4, 100%), meningeal enhancement (3/3, 100%), and suspected intracranial hypertension (4/4, 100%) completely resolved.

Immunosuppressive treatment in these dogs substantially decreased lesion number and size and resolved initial MRI features and associated findings, including lesional contrast enhancement, perilesional edema, mass effect, meningeal enhancement, and suspected intracranial hypertension. Agreement between clinical and MRI neurolocalization was observed in 50% (4/8) of cases, suggesting that residual lesions in some dogs may have had limited clinical relevance.

Differences were observed between the 2/8 (25%) dogs with persistent neurological signs and the 6/8 (75%) dogs with clinical resolution. The 2/2 (100%) dogs with persistent neurological signs exhibited persistence of the same lesions, with a decrease in size and T2W-FLAIR signal suppression. Among those with clinical resolution, 2/6 (33%) achieved complete lesional resolution, and 2/6 (33%) experienced partial resolution; 1/6 (17%) dog showed T2W-FLAIR signal suppression.

At the time of the control MRI, dogs with persistent neurological signs exhibited less favorable lesional response to immunosuppressive treatment, with more necrosis (T2W-FLAIR signal suppression), whereas those with clinical resolution showed a more favorable lesional response, albeit often without complete lesional resolution.

3.5 | Relapse MRI Findings (Tables 2–4, 6 and Figures 1–4)

The median interval between initial and relapse MRI was 259 days (range, 31–876), extending 49 days beyond the previously reported median relapse delay of 210 days after diagnosis [24, 25]. Ongoing immunosuppressive treatment was present in 13/18 (72%) dogs. At relapse, 89% (16/18) of dogs exhibited clinical signs, predominantly acute (9/18, 50%) or subacute (5/18, 28%), with a median duration of 3 days, a marked decrease from 27.5 days at initial diagnosis, representing an 89% change. The 3/18 (17%) dogs without neurological signs still were receiving immunosuppressive treatment (prednisolone and cytosine arabinoside). Agreement between clinical and MRI neurolocalization was observed in 14/18 (78%), suggesting that some residual lesions may lack clinical relevance (Figure 5).

Notable differences from the initial MRI findings were observed, highlighting several trends. Among the 8 dogs with a relapse delay <157 days (8/18, 44%), all (8/8, 100%) exhibited stable or decreased lesion numbers. The median lesion number decreased from 3.5 to 3 per dog, a 14% decrease. None developed new lesions or achieved complete lesional remission. Most (7/8, 88%) demonstrated stable or increased sizes of some or all initial lesions. Lesional contrast enhancement was frequent in enlarged lesions (5/6, 83%) but rare in those that decreased in size (1/4, 25%). Perilesional edema was common in enlarged lesions (5/6, 83%) but absent in those that decreased in size. Clinical resolution of neurological signs between initial and relapse MRI was uncommon (2/8, 25%).

Among the 10 dogs with a relapse delay >233 days (10/18, 56%), 9/10 (90%) had stable or increased lesion numbers. The median lesion number increased from 3.5 to 4 per dog, a 14% increase. All (10/10, 100%) developed new lesions, with frequent lesional contrast enhancement (8/10, 80%) and perilesional edema (6/10, 60%). Most (9/10, 90%) exhibited a disappearance or decrease in the size of some or all initial lesions. Half (5/10, 50%) showed an increase in the size of some residual lesions, with lesional contrast enhancement and perilesional edema common (3/5, 60%) in some or all enlarged lesions but uncommon (1/5, 20%) in those that decreased in size. Resolution of neurological signs between initial and relapse MRI was achieved in 3/5 (60%) dogs of this subgroup. The remaining (5/10, 50%) displayed no residual lesions enlargement, and 2/5 (20%) achieved complete lesional resolution. Residual lesions that decreased in size exhibited no contrast enhancement or perilesional edema. All dogs (5/5, 100%) in this subgroup achieved complete resolution of neurological signs between initial and relapse MRI. No significant association was found between these two groups and relapse delay.

Changes in lesion distribution also were observed. Forebrain lesion number increased slightly by 5 percentage points (pp), whereas hindbrain lesion number decreased moderately by 16 pp. Among forebrain lesions, telencephalic lesion number increased slightly by 6 pp, with parietal lesions increasing markedly by 34 pp, whereas diencephalic lesion number decreased moderately by 17 pp. Three more dogs developed lesional T2W-FLAIR signal suppression at relapse, increasing from 5/18 (28%) to 8/18 (44%), reflecting a 16 pp increase. Suspected intracranial hypertension decreased by 17 pp, from 9/18 (50%) to 6/18 (33%) at relapse. Lesion distribution, localization, and lesional MRI features and associated findings were consistent with those expected in MUO.

The 3/18 (17%) dogs with lesional relapse but no neurological signs were further analyzed. All (3/3, 100%) were still undergoing

TABLE 3 | Descriptive statistics for MUO lesions in terms of distribution and localization on initial and relapse MRI, and evolution quantification.

n = 18	Initial diagnosis	Relapse	Evolution
Lesion distribution and localization			
Multifocal	16/18 (89%)	16/18 (89%)	0 pp
Forebrain	16/16 (100%)	16/16 (100%)	0 pp
Hindbrain	6/16 (38%)	4/16 (25%)	−13 pp
Focal	2/18 (11%)	2/18 (11%)	0 pp
Hindbrain	2/2 (100%)	1/2 (50%)	−50 pp
Forebrain	0/2 (0%)	1/2 (50%)	+50 pp
Forebrain	16/18 (89%)	17/18 (94%)	+5 pp
Telencephalon	15/16 (94%)	16/17 (94%)	0 pp
Diencephalon	10/16 (63%)	7/17 (41%)	−22 pp
Hindbrain	8/18 (44%)	5/18 (28%)	−16 pp
Pons	8/8 (100%)	5/5 (100%)	0 pp
Cerebellum	2/8 (25%)	2/5 (40%)	+15 pp
Medulla oblongata	2/8 (25%)	0/5 (0%)	−25 pp
Telencephalon	15/18 (83%)	16/18 (89%)	+6 pp
Frontal lobe	11/15 (73%)	12/16 (75%)	+2 pp
Parietal lobe	9/15 (60%)	15/16 (94%)	+34 pp
Occipital lobe	7/15 (47%)	8/16 (50%)	+3 pp
Temporal lobe	6/15 (40%)	4/16 (25%)	−15 pp
Diencephalon	10/18 (56%)	7/18 (39%)	−17 pp
Thalamus	*9/10 (90%)*	*7/7 (100%)*	*+10 pp*
Optic chiasma	*1/10 (10%)*	*0/7 (0%)*	*−10 pp*

Abbreviations: MRI, magnetic resonance imaging; MUO, meningoencephalomyelitis of unknown origin; pp, percentage point; T1W, T1-weighted; T2W, T2-weighted; T2W-FLAIR, T2-weighted fluid-attenuated inversion recovery.

TABLE 4 | Descriptive statistics for MUO lesions in terms of number, MRI features, and associated findings on initial and relapse MRI, and evolution quantification.

n = 18	Initial diagnosis	Relapse < 157 days (*n* = 8)	Evolution	Relapse > 233 days (*n* = 10)	Evolution
Median lesion number (min–max)	3, 5 (1–5)	3 (1–5)	−14%	4 (1–6)	+14%

n = 18	Initial diagnosis	Relapse	Evolution
Lesional MRI features and associated findings			
T2W-FLAIR signal suppression	5/18 (28%)	8/18 (44%)	+16 pp
Meningeal enhancement	4/18 (22%)	4/18 (22%)	0 pp
Mass effect	11/18 (61%)	10/18 (55%)	−6 pp
Suspected intracranial hypertension	9/18 (50%)	6/18 (33%)	−17 pp

Abbreviations: MRI, magnetic resonance imaging; MUO, meningoencephalomyelitis of unknown origin; pp, percentage point; T1W, T1-weighted; T2W, T2-weighted; T2W-FLAIR, T2-weighted fluid-attenuated inversion recovery.

immunosuppressive treatment (prednisolone and cytosine arabinoside). No specific evolution in lesional MRI features or associated findings was noted. One dog (1/3, 33%) belonged to the < 157-day relapse delay group, exhibiting a stable number of lesions with no new lesions. The remaining two (2/3, 67%) had a > 233-day relapse delay, with stable or increased lesion number

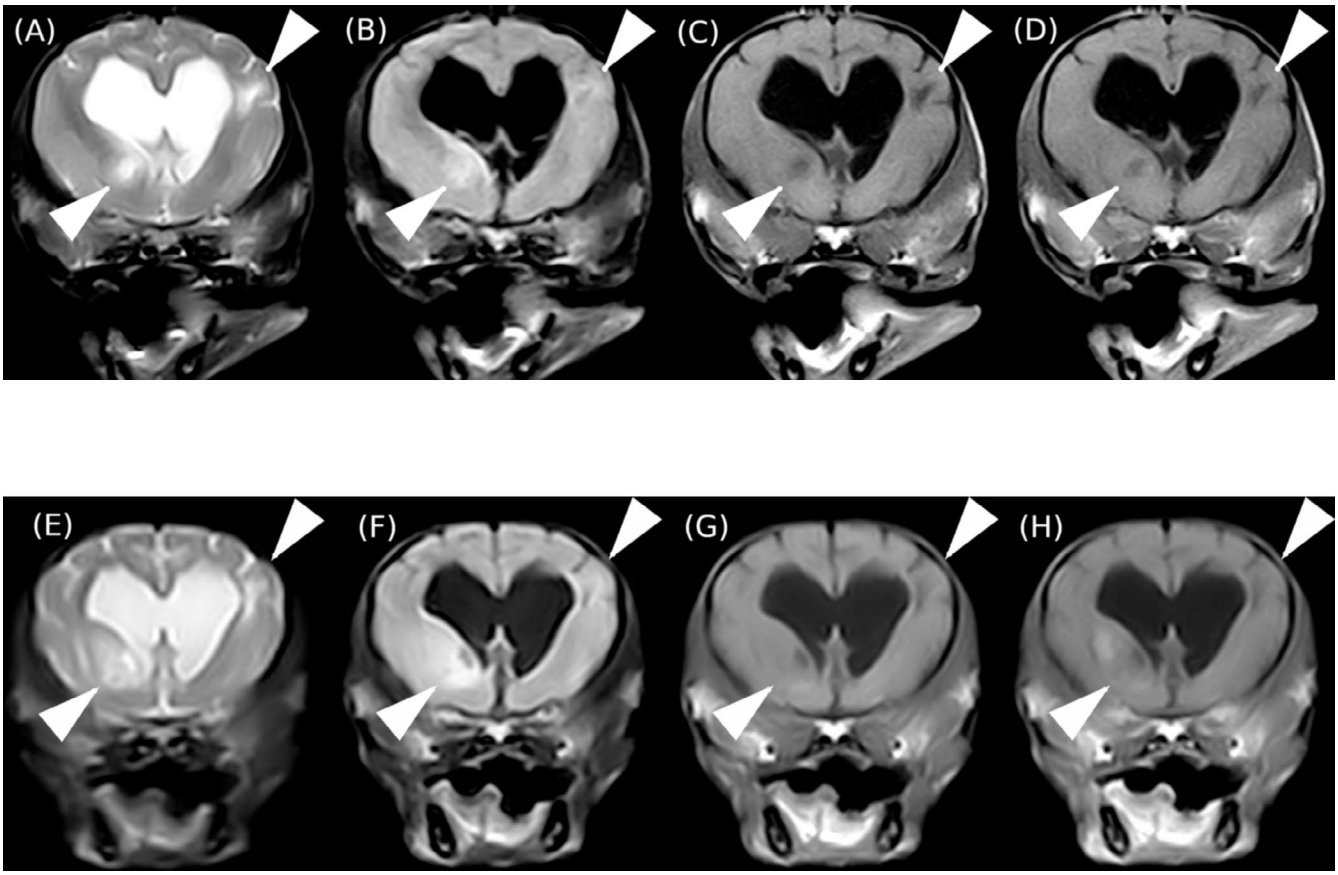

FIGURE 1 | Example of evolution between initial and relapse MRI of multifocal MUO lesions with a relapse delay of less than 6 months, characterized by partial lesional response to immunosuppressive therapy with active/inflammatory residual lesions. Transverse T2W (A, E), T2W-FLAIR (B, F), T1W (C, G), T1W + C (D, H) sequences of the brain of a 5-year-old male Chihuahua at the level of the parietal and temporal lobes at the time of initial (A–D) (T0) and relapse (E–H) (T0 + 125d) MRI. (A–D) Initially, there were multifocal T2W hyperintense lesions in the left parietal lobe and in the right thalamus (arrowheads). The left parietal lobe lesion showed a necrotic focus (T2W-FLAIR signal suppression) and no evidence of contrast enhancement or perilesional edema. The right thalamic lesion showed no evidence of a necrotic focus and was discretely peripherally enhancing, with discrete perilesional edema. (E–H) At relapse, the left parietal lesion was stable. The right thalamic lesion was enlarged, with the appearance of a necrotic focus and evidence of lesional contrast enhancement and perilesional edema. d, day; MRI, magnetic resonance imaging; MUO, meningoencephalomyelitis of unknown origin; T1W, T1-weighted; T1W + C, T1-weighted after contrast media injection; T2W, T2-weighted; T2W-FLAIR, T2-weighted fluid-attenuated inversion recovery.

and new lesions. One was categorized in the subgroup showing some enlarged residual lesions, whereas the other belonged to the group showing lesional resolution or residual lesions that had decreased in size. All dogs (3/3, 100%) exhibited lesional contrast enhancement in both enlarged and new lesions, without perilesional edema, mass effect, or suspected intracranial hypertension.

4 | Discussion

Before a relapse delay of 5.2 months (157 days), lesion number remained stable or decreased, with no new lesions and incomplete resolution of the initial lesions. Most residual lesions were either enlarged or stable in size, with frequent lesional contrast enhancement and perilesional edema in the enlarged lesions. This finding suggests a partial lesional response to immunosuppressive treatment, with persistent active residual lesions and no new lesion development, indicating probable absence of remission of the initial pathologic process. A minority of dogs achieved resolution of neurological signs between the initial and relapse MRI, supporting this hypothesis. After a relapse delay of 7.7 months (233 days), lesion number was primarily stable or increased, with new lesions in all dogs. Lesional contrast enhancement and perilesional edema were frequent in new lesions. Half of these dogs exhibited an increase in the size of some residual lesions, with frequent lesional contrast enhancement and perilesional edema in enlarged lesions, whereas lesions that decreased in size rarely exhibited lesional contrast enhancement and no perilesional edema. These findings suggest a partial lesional response to immunosuppressive treatment, with active residual lesions associated with new lesion development, indicating probable absence of remission of the initial pathologic process with relapse of the same type of lesion in a different brain region. However, most dogs in this subgroup achieved resolution of neurological signs between initial and relapse MRI. In the remaining half, all initial lesions disappeared or decreased in size, with no lesional contrast enhancement or perilesional edema. This finding suggests a good lesional response to immunosuppressive treatment, with initial lesion resolution or cicatricial gliosis associated with new lesion development, indicating probable remission of the initial pathologic process with relapse of

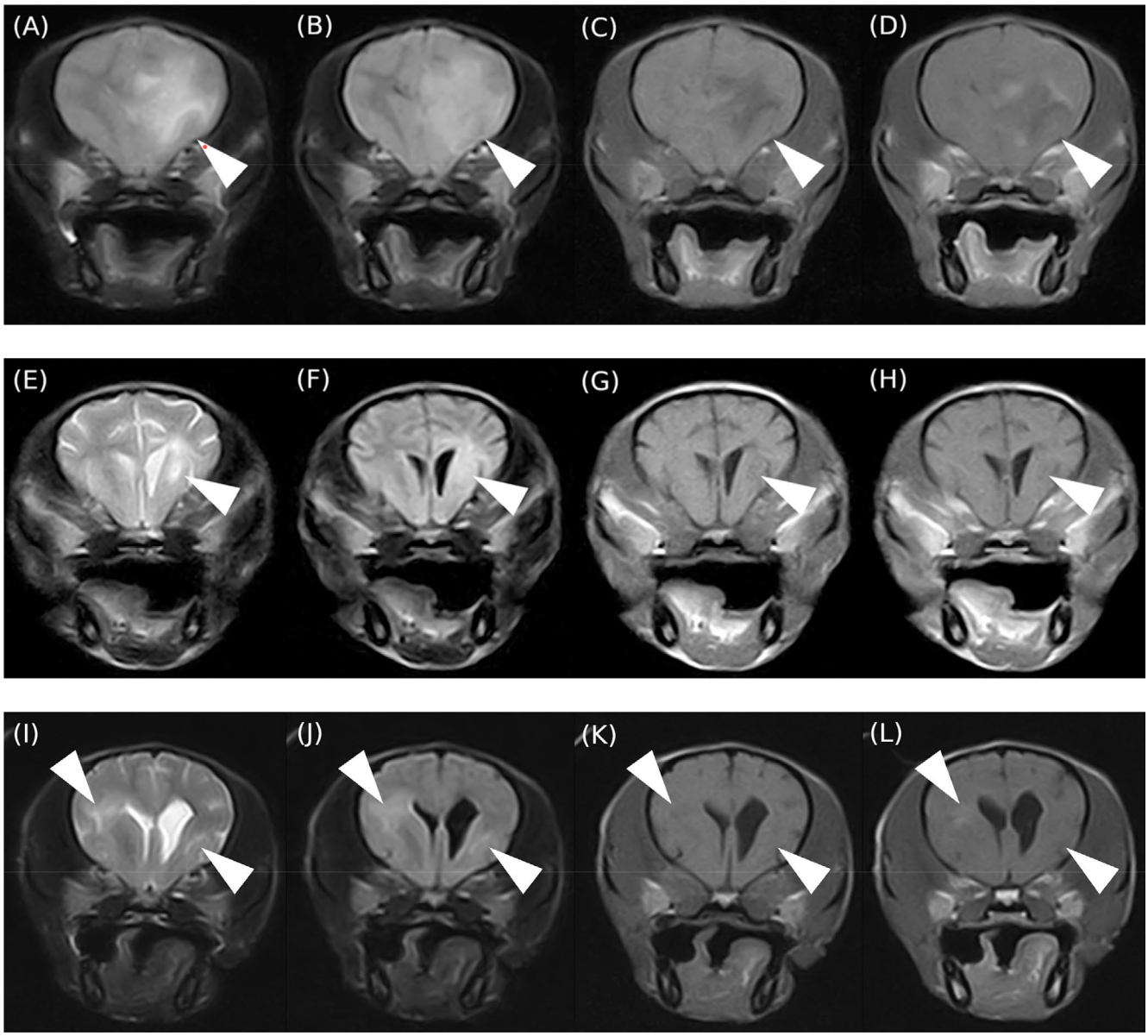

FIGURE 2 | Example of MUO lesion evolution between initial, control, and relapse MRI of multifocal MUO lesions with a relapse delay exceeding 6 months, characterized by a good lesional response to immunosuppressive therapy with resolution of the initial lesions and/or cicatricial gliosis of the residual lesions associated with new lesion development. Transverse T2W (A, E, I), T2W-FLAIR (B, F, J), T1W (C, G, K), T1W + C (D, H, L) sequences of the brain of a 1-year-old female Pomeranian at the level of the fronto-parieto-temporal lobe junction at the time of initial (A–D) (T0), control (E–H) (T0 + 105d), and relapse (I–L) (T0 + 446d) MRI. (A–D) Initially, there was a T2W hyperintense lesion without a necrotic area (no T2W-FLAIR signal suppression) at the left fronto-temporal lobe junction, with heterogeneous peripheral contrast enhancement (arrowheads) surrounded by perilesional edema and associated with suspected intracranial hypertension (mass effect on the cerebral falx and attenuation of the cerebral sulci). (E–H) On control MRI, after immunosuppressive treatment, the lesion decreased in size (first arrowheads) without evidence of lesional contrast enhancement or intracranial hypertension (midline position of the cerebral falx, visible cerebral sulci). (I–L) At relapse, the initial lesion had almost disappeared (first arrowheads), and a new T2W hyperintense lesion without evidence of necrosis and discretely enhancing at the right fronto-parieto-temporal lobe junction (second arrowheads), with perilesional edema and intracranial hypertension (attenuation of cerebral sulci) was present. d, day, MRI, magnetic resonance imaging; MUO, meningoencephalomyelitis of unknown origin; T1W, T1-weighted; T1W + C, T1-weighted after contrast media injection; T2W, T2-weighted; T2W-FLAIR, T2-weighted fluid-attenuated inversion recovery.

the same type of lesion in a different brain region. All dogs in this subgroup achieved resolution of neurological signs between the initial and relapse MRI, supporting this hypothesis.

Thus, before a relapse delay of approximately 6 months, dogs tended to experience an absence of remission of the initial pathologic process. Consequently, repeat MRI provides little additional diagnostic or clinical value. Beyond this period, two possibilities emerge: all dogs appear to relapse in a different brain region, but some tend to experience an absence of remission of the initial pathologic process, whereas others appear to achieve remission. Therefore, repeat MRI at the time of relapse seems to be of high diagnostic and clinical value, helping identify new lesions, characterizing the underlying

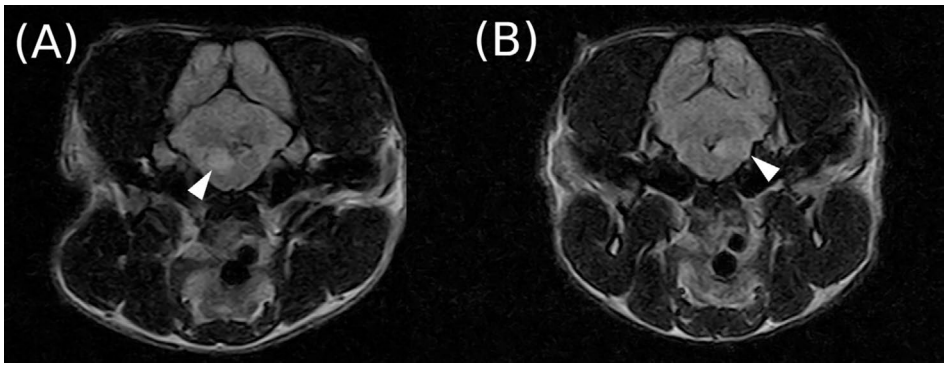

FIGURE 3 | Example of evolution between initial and relapse MRI of focal MUO lesion with a relapse delay of more than 6 months characterized by lesional resolution with immunosuppressive therapy associated with new lesion development. Transverse T2W-FLAIR (A, B) sequences of the brain of a 3-year-old female French bulldog at the level of the pons at the time of initial (A) (T0) and relapse (B) (T0 + 291d) MRI. (A) Initially, there was a hyperintense lesion at the right aspect of the pons (arrowheads), which had disappeared with immunosuppressive treatment on control MRI (not shown). (B) At relapse, a new hyperintense lesion was seen at the left aspect of the pons (arrowheads). d, day; MRI, magnetic resonance imaging; MUO, meningoencephalomyelitis of unknown origin; T2W-FLAIR, T2-weighted fluid-attenuated inversion recovery.

TABLE 5 | Descriptive statistics for MUO lesions in terms of number, MRI features, and associated findings on initial and control MRI, and evolution quantification.

n = 8	Initial diagnosis	Control	Evolution
Median lesion number (min–max)	3, 5 (0–4)	1 (0–4)	−71%
Lesional MRI features and associated findings			
T2W-FLAIR signal suppression	3/8 (37%)	3/8 (37%)	0 pp
Mass effect	4/8 (50%)	0/8 (0%)	−50 pp
Meningeal enhancement	3/8 (37%)	0/8 (0%)	−37 pp
Suspected intracranial hypertension	4/8 (50%)	0/8 (0%)	−50 pp

Abbreviations: MRI, magnetic resonance imaging; MUO, meningoencephalomyelitis of unknown origin; pp, percentage point; T1W, T1-weighted; T2W, T2-weighted; T2W-FLAIR, T2-weighted fluid-attenuated inversion recovery.

pathologic process, and potentially impacting treatment decisions (Figure 5).

Many intracranial pathologic processes result in some degree of disruption of the blood–brain barrier (BBB) because of damage to brain capillaries, often allowing intralesional contrast medium accumulation after extravasation from the vasculature (lesional contrast enhancement) and resulting in fluid leakage into the extracellular space (perilesional edema) [7, 17, 26]. Histopathologic analysis indicates that the predominant pattern in inflammatory brain lesions, including MUO, is perivascular cuffing with inflammatory cells [15, 22], which is associated with BBB disruption in mice with experimentally induced allergic encephalomyelitis [32, 33]. Thus, the intensity of lesion inflammation may correlate with lesional contrast enhancement and perilesional edema on MRI. These observations were further supported in our study through the evolution of lesional contrast enhancement and perilesional edema. These features systematically resolved on control MRI (performed between initial and relapse MRI in some dogs) when initially present, and tended to be present at relapse in both enlarged and new lesions and to disappear in lesions that decreased in size. In addition, a moderate discrepancy between clinical and imaging neurolocalization at the time of control and relapse MRI suggested that some of the lesions were minimally active to non-active (e.g., cicatricial gliosis). Conversely, lesions with contrast enhancement or perilesional edema at relapse were likely active lesions.

Surprisingly, no Pugs, a breed known to be highly predisposed to MUO, particularly NE [6, 19, 20, 34–36], met the inclusion criteria. Pugs were underrepresented in the client-owned dog population at our institution and experienced severe clinical signs at the time of relapse, leading to death or euthanasia. This observation is consistent with a recent study [25] showing that Pugs were less likely than other breeds to survive beyond 6 months post-diagnosis. The most represented breeds in our study were Chihuahua, followed by French Bulldog and Yorkshire Terrier, all of which are reported to be predisposed to MUO [2]. Granulomatous meningoencephalitis can occur in any breed, typically in smaller breeds, but Chihuahua [37], French Bulldog [38], and Yorkshire Terrier [21, 39–42] are among those reported to be affected by NE [19].

Given this breed-related predisposition, it is worth considering whether NE relapses more frequently than GME, particularly because NE generally has a worse prognosis [4, 7, 17]. Additionally, MRI-detected MUO lesions typically involve the forebrain in NME, with severe parietal and occipital cortex lesions, whereas NLE predominantly affects the forebrain and brainstem. In our study, forebrain lesions were common at initial diagnosis and relapse, with lesion number trends showing a moderate 16 pp decrease in the hindbrain but a significant 34 pp increase in the parietal lobe at relapse. Moreover, the proportion of dogs with T2W-FLAIR signal suppression, indicative of necrosis and possibly associated with NE, increased by 16 pp, affecting nearly half of the dogs at relapse. However, a recent study indicated the

TABLE 6 | Lesional contrast enhancement and perilesional edema associated with MUO lesion size on control and relapse MRI.

	Control ($n=8$)		Relapse delay < 157d ($n=8$)			Relapse delay > 233d ($n=10$)		
Dogs with	**Contrast enhancement**	**Perilesional edema**		**Contrast enhancement**	**Perilesional edema**		**Contrast enhancement**	**Perilesional edema**
New lesions	$n=0$	/	/	$n=0$	/	$n=10$	8/10 (80%)	6/10 (60%)
Enlarged lesions	$n=0$	/	/	$n=6$	5/6 (83%)	$n=5$	3/5 (60%)	3/5 (60%)
Similar sized lesions	$n=0$	/	/	$n=2$	1/2 (50%)	$n=1$	0/1 (0%)	0/1 (0%)
Decreased in size lesions	$n=6$	0/6 (0%)	0/6 (0%)	$n=4$	1/4 (25%)	$n=7$	1/7 (14%)	0/7 (0%)

Abbreviations: d, day; MRI, magnetic resonance imaging; MUO, meningoencephalomyelitis of unknown origin.

potential coexistence of GME and NE in the same dog, limiting the clinical value of distinguishing the different MUO types and subtypes by antemortem diagnostic imaging [43].

The remaining lesion characteristics, such as distribution and signal aspect, were consistent with previously reported MUO features [4, 7, 17] and their evolution was unremarkable. However, a selection bias may be present, because atypical presentations of MUO were excluded in our study to improve the consensus of the initial diagnosis. Regarding suspected intracranial hypertension, a 17 pp decrease in number at relapse was observed. Several hypotheses can be considered, including the higher proportion of dogs on anti-inflammatory medications and with necrotic areas at relapse.

The median age of patients at diagnosis was 3.5 years, and no dogs weighed >12.5 kg. This predisposition of young adult small dogs is consistent with previously reported findings [2]. Although it was widely believed that GME exhibits a female predominance, recent studies have reported no significant female-to-male ratio difference [1, 2, 4, 6]. However, the female-to-male ratio in our study was 2:1, potentially suggesting an increased relapse risk in females.

The median interval between initial and relapse MRI in our study was 259 days. Previous studies reported a median relapse delay of 210 days after diagnosis [24, 25], shorter than the median relapse delay observed in our study. The median duration of clinical signs between clinical relapse and relapse MRI in our study was only 3 days, too brief to account for this difference.

All dogs in our study were receiving multimodal immunosuppressive treatment, which was considered the gold standard at the time of the study. However, a recent review failed to demonstrate a significant advantage over glucocorticoid treatment alone [44]. Nevertheless, multimodal immunosuppressive treatment allows for glucocorticoid dose reduction, consequently mitigating the adverse effects associated with high-dose glucocorticoid administration. In our study, glucocorticoid treatment was combined with cytosine arabinoside or cyclosporine, but alternative treatments also have shown efficacy [44].

Some dogs in our study underwent control MRI, CSF analysis, or both during immunosuppressive treatment, based on a previous study [24], that demonstrated that: (1) resolution of MRI abnormalities 3 months after diagnosis is associated with favorable outcome, (2) persistent CSF abnormalities at 3 months or treatment discontinuation before MRI resolution increases relapse risk, and (3) MRI and CSF analysis together provide higher sensitivity in predicting relapse than either modality alone [24]. This intermediate MRI enabled confirmation of the presumptive MUO diagnosis because all dogs exhibited lesion improvement or resolution on control MRI, and all dogs initially suspected of intracranial hypertension showed resolution. However, dogs that relapsed before 3 months or those whose owners did not consent to control examinations did not benefit from this additional monitoring.

A recent study [25] identified risk factors associated with relapse, including incomplete resolution of clinical signs within 6 months of diagnosis, a higher neurodisability scale score [45],

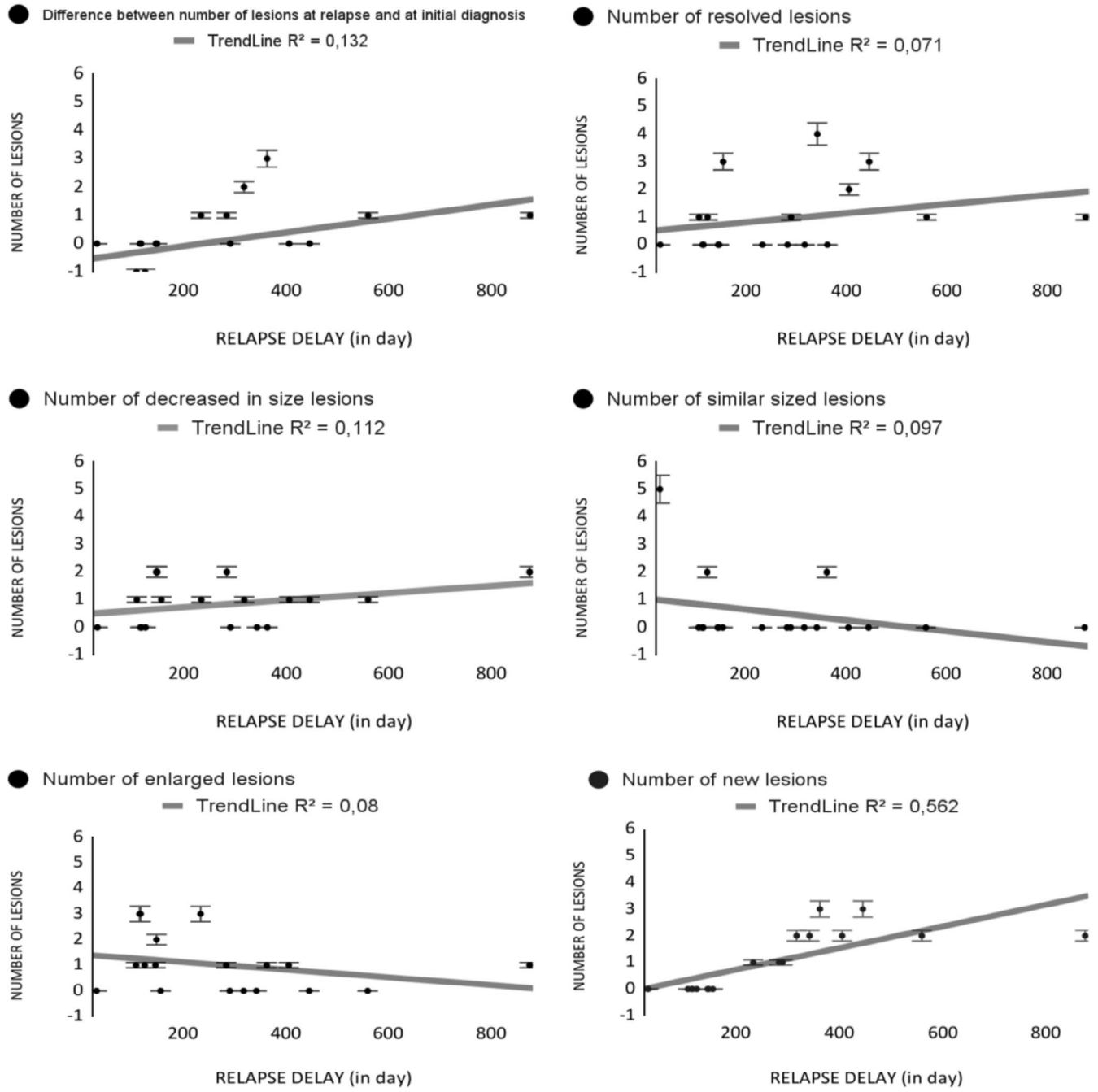

FIGURE 4 | Trend line for the following variables: Difference between the number of lesions at relapse and at initial diagnosis, and the number of resolved, decreased in size, similar sized, enlarged, and new lesions at relapse.

and prolonged duration of clinical signs before presentation. Similarly, in our study, the majority of dogs initially exhibited a chronic presentation, and nearly half did not achieve complete resolution of their initial clinical signs.

Our study had some limitations. As a retrospective study based on a cohort of 18 dogs, this design allowed for the inclusion of cases from a large patient pool group, which was deemed an acceptable study population given the inclusion criteria. However, it may have introduced inaccuracies in data collection or selection bias. Another limitation was that our images were acquired using a low-field MRI scanner, and the applicability of our findings to high-field MRI remains to be determined. The low magnetic field strength used in our study affected image quality, particularly the signal-to-noise ratio. Additionally, a low-field MRI scanner is less sensitive for detecting hemorrhagic lesions and decreases discrimination of gadolinium-enhancing lesions. We did not opt to increase the gadolinium dose to 0.15 mmol/kg instead of the standard 0.1 mmol/kg, as suggested by some authors. However, the impact on diagnostic accuracy remains unclear, and overall, the sensitivity of low-field and high-field MRI scanners for detecting the disease itself appears to be comparable [17, 46–48]. Some dogs were receiving immunosuppressive treatment at the time of initial MRI diagnosis, which may have influenced lesion characteristics on these initial studies. This factor was not considered an exclusion criterion because

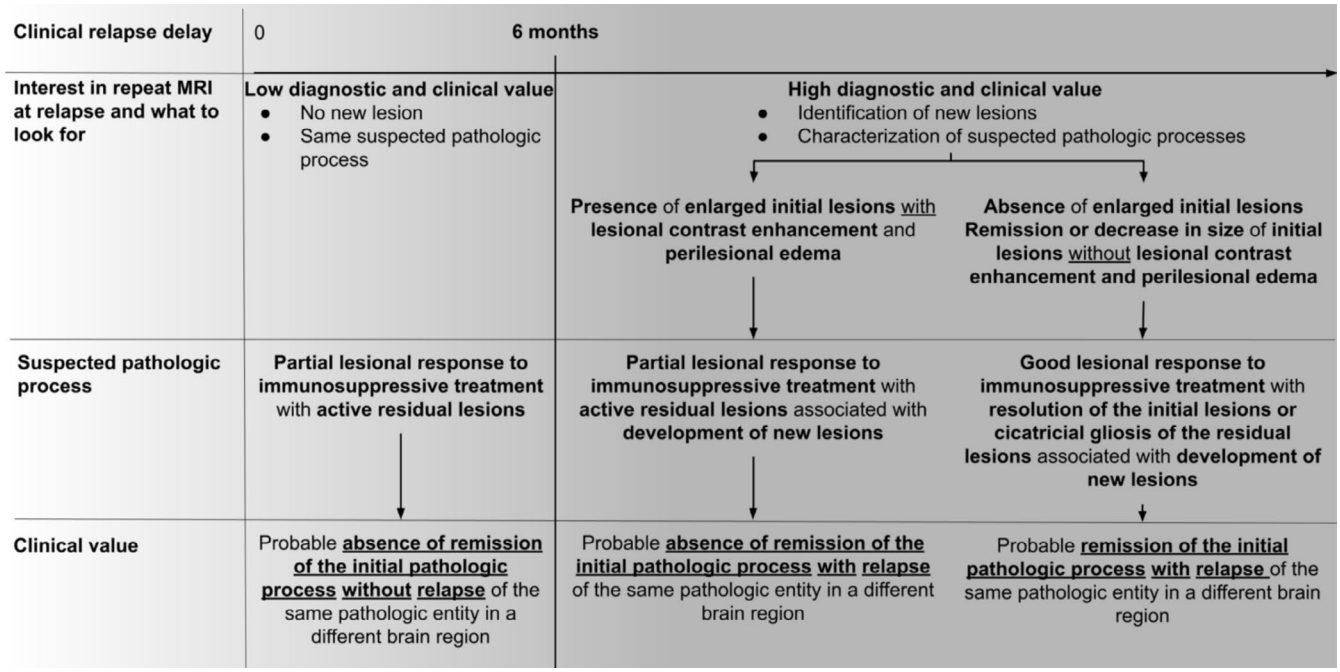

FIGURE 5 | Summary of key findings.

the images were compared with control and relapse MRIs, which often were acquired under ongoing immunosuppressive treatment. Additionally, it was deemed ethically inappropriate to discontinue treatment prescribed by the referring clinician and delay MRI for several days, given the severity of the disease. Finally, we did not obtain a definitive diagnosis by histopathology from antemortem biopsy specimens or postmortem brain samples in any of the dogs with a presumptive diagnosis of MUO. As a result, the diagnosis remained presumptive, without confirmation or characterization of the specific type and subtype involved in relapse.

In conclusion, our findings suggest that before a relapse delay of approximately 6 months, the suspected pathologic process correlates with partial lesional response to immunosuppressive treatment, characterized by persistent active residual lesions and no new lesion development, indicating a probable absence of remission of the initial pathologic process. Consequently, repeat MRI provides limited additional diagnostic or clinical value. After a relapse delay of approximately 6 months, two possible pathologic processes emerge: new lesion development associated with partial lesional response (some active residual lesions) or a good lesional response (initial lesions resolution or cicatricial gliosis) to immunosuppressive treatment. This finding suggests probable relapse of the same pathologic entity in a different brain region, with or without remission of the initial pathologic process. Therefore, repeat MRI at the time of relapse seems to be of high diagnostic and clinical value, enabling the identification of new lesions and characterization of the suspected pathologic processes, potentially impacting treatment decisions. However, additional studies are needed to confirm these findings, which could enhance understanding of the pathologic process of MUO at the time of clinical relapse, determine whether these results could lead to treatment recommendations to improve survival, and clarify whether a specific type or subtype of MUO is preferentially involved in relapse, which would aid in its antemortem characterization.

Disclosure

Authors declare no off-label use of antimicrobials.

Ethics Statement

Authors declare no Institutional Animal Care and Use Committee or other approval was needed. Authors declare human ethics approval was not needed.

Conflicts of Interest

The authors declare no conflicts of interest.

References

1. L. R. Talarico and S. J. Schatzberg, "Idiopathic Granulomatous and Necrotising Inflammatory Disorders of the Canine Central Nervous System: A Review and Future Perspectives," *Journal of Small Animal Practice* 51, no. 3 (2010): 138–149, https://doi.org/10.1111/j.1748-5827.2009.00823.x.

2. N. Granger, P. M. Smith, and N. D. Jeffery, "Clinical Findings and Treatment of Non-Infectious Meningoencephalomyelitis in Dogs: A Systematic Review of 457 Published Cases From 1962 to 2008," *Veterinary Journal* 184, no. 3 (2010): 290–297, https://doi.org/10.1016/j.tvjl.2009.03.031.

3. J. R. Coates and N. D. Jeffery, "Perspectives on Meningoencephalomyelitis of Unknown Origin," *Veterinary Clinics of North America: Small Animal Practice* 44, no. 6 (2014): 1157–1185, https://doi.org/10.1016/j.cvsm.2014.07.009.

4. I. Cornelis, L. Van Ham, I. Gielen, et al., "Clinical Presentation, Diagnostic Findings, Prognostic Factors, Treatment and Outcome in Dogs With Meningoencephalomyelitis of Unknown Origin: A Review,"

Veterinary Journal 244 (2019): 37–44, https://doi.org/10.1016/j.tvjl.2018.12.007.

5. J. J. Cooper, S. J. Schatzberg, K. M. Vernau, et al., "Necrotizing Meningoencephalitis in Atypical Dog Breeds: A Case Series and Literature Review," *Journal of Veterinary Internal Medicine* 28, no. 1 (2014): 198–203, https://doi.org/10.1111/jvim.12233.

6. J. M. Levine, G. T. Fosgate, B. Porter, S. J. Schatzberg, and K. Greer, "Epidemiology of Necrotizing Meningoencephalitis in Pug Dogs," *Journal of Veterinary Internal Medicine* 22, no. 4 (2008): 961–968, https://doi.org/10.1111/j.1939-1676.2008.0137.x.

7. C. W. Dewey and R. C. da Costa, eds., *Practical Guide to Canine and Feline Neurology*, Third ed. (Wiley-Blackwell, 2016).

8. A. de Lahunta, *De Lahunta's Veterinary Neuroanatomy and Clinical Neurology*, 5th ed. (Elsevier Inc, 2020).

9. P. Menaut, J. Landart, S. Behr, D. Lanore, and C. Trumel, "Treatment of 11 Dogs With Meningoencephalomyelitis of Unknown Origin With a Combination of Prednisolone and Cytosine Arabinoside," *Veterinary Record* 162, no. 8 (2008): 241–245, https://doi.org/10.1136/vr.162.8.241.

10. P. D. Koblik, R. A. Lecouteur, R. J. Higgins, et al., "Modification and Application of a Pelorus Mark III Stereotactic System for Ct-Guided Brain Biopsy in 50 Dogs," *Veterinary Radiology & Ultrasound* 40, no. 5 (1999): 424–433, https://doi.org/10.1111/j.1740-8261.1999.tb00370.x.

11. P. Moissonnier, S. Blot, P. Devauchelle, et al., "Stereotactic CT-Guided Brain Biopsy in the Dog," *Journal of Small Animal Practice* 43, no. 3 (2002): 115–123, https://doi.org/10.1111/j.1748-5827.2002.tb00041.x.

12. J. H. Rossmeisl, R. T. Andriani, T. E. Cecere, et al., "Frame-Based Stereotactic Biopsy of Canine Brain Masses: Technique and Clinical Results in 26 Cases," *Frontiers in Veterinary Science* 2 (2015): 20, https://doi.org/10.3389/fvets.2015.00020.

13. S. Gutmann, C. Tästensen, I. C. Böttcher, et al., "Clinical Use of a New Frameless Optical Neuronavigation System for Brain Biopsies: 10 Cases (2013–2020)," *Journal of Small Animal Practice* 63, no. 6 (2022): 468–481, https://doi.org/10.1111/jsap.13482.

14. L. Gaitero, S. J. Russell, G. Monteith, and J. LaMarre, "Expression of microRNAs miR-21 and miR-181c in Cerebrospinal Fluid and Serum in Canine Meningoencephalomyelitis of Unknown Origin," *Veterinary Journal* 216 (2016): 122–124, https://doi.org/10.1016/j.tvjl.2016.07.014.

15. K. Uchida, E. Park, M. Tsuboi, J. K. Chambers, and H. Nakayama, "Pathological and Immunological Features of Canine Necrotising Meningoencephalitis and Granulomatous Meningoencephalitis," *Veterinary Journal* 213 (2016): 72–77, https://doi.org/10.1016/j.tvjl.2016.05.002.

16. E. Andersen-Ranberg, M. Berendt, and H. Gredal, "Biomarkers of Non-Infectious Inflammatory CNS Diseases in Dogs—Where Are We Now? Part I: Meningoencephalitis of Unknown Origin," *Veterinary Journal* 273 (2021): 105678, https://doi.org/10.1016/j.tvjl.2021.105678.

17. W. Maï, *Diagnostic MRI in Dogs and Cats* (CRC Press, 2018).

18. G. B. Cherubini, S. R. Platt, T. J. Anderson, et al., "Characteristics of Magnetic Resonance Images of Granulomatous Meningoencephalomyelitis in 11 Dogs," *Veterinary Record* 159, no. 4 (2006): 110–115, https://doi.org/10.1136/vr.159.4.110.

19. T. Flegel, "Breed-Specific Magnetic Resonance Imaging Characteristics of Necrotizing Encephalitis in Dogs," *Frontiers in Veterinary Science* 4 (2017): 203, https://doi.org/10.3389/fvets.2017.00203.

20. B. D. Young, J. M. Levine, G. T. Fosgate, et al., "Magnetic Resonance Imaging Characteristics of Necrotizing Meningoencephalitis in Pug Dogs," *Journal of Veterinary Internal Medicine* 23, no. 3 (2009): 527–535, https://doi.org/10.1111/j.1939-1676.2009.0306.x.

21. F. Von Praun, K. Matiasek, V. Grevel, et al., "Magnetic Resonance Imaging and Pathologic Findings Associated With Necrotizing Encephalitis in Two Yorkshire Terriers," *Veterinary Radiology & Ultrasound* 47, no. 3 (2006): 260–264, https://doi.org/10.1111/j.1740-8261.2006.00137.x.

22. M. VanDe Velde, R. J. Higgins, and A. S. L. Oevermann, *Veterinary Neuropathology: Essentials of Theory and Practice* (Wiley-Blackwell, 2012).

23. A. Ostrager, R. T. Bentley, M. J. Lewis, and G. E. Moore, "Survival in Dogs With Meningoencephalomyelitis of Unknown Etiology With and Without Lesions Detected by Magnetic Resonance Imaging," *Journal of Veterinary Internal Medicine* 38, no. 4 (2024): jvim.17109, https://doi.org/10.1111/jvim.17109.

24. M. Lowrie, P. M. Smith, and L. Garosi, "Meningoencephalitis of Unknown Origin: Investigation of Prognostic Factors and Outcome Using a Standard Treatment Protocol," *Veterinary Record* 172, no. 20 (2013): 527, https://doi.org/10.1136/vr.101431.

25. R. Gonçalves, S. De Decker, G. Walmsley, et al., "Prognosis in Meningoencephalitis of Unknown Origin in Dogs: Risk Factors Associated With Survival, Clinical Relapse, and Long-Term Disability," *Journal of Veterinary Internal Medicine* 38 (2024): 1583–1590, https://doi.org/10.1111/jvim.17037.

26. D. E. Thrall, *Textbook of Veterinary Diagnostic Radiology*, Seventh ed. (Elsevier, 2018).

27. M. J. Lewis, N. J. Olby, P. J. Early, et al., "Clinical and Diagnostic Imaging Features of Brain Herniation in Dogs and Cats," *Journal of Veterinary Internal Medicine* 30, no. 5 (2016): 1672–1680, https://doi.org/10.1111/jvim.14526.

28. S. Giannasi, Y. Kani, F. C. Hsu, and J. H. Rossmeisl, "Comparison of Direct Measurement of Intracranial Pressures and Presumptive Clinical and Magnetic Resonance Imaging Indicators of Intracranial Hypertension in Dogs With Brain Tumors," *Journal of Veterinary Internal Medicine* 34, no. 4 (2020): 1514–1523, https://doi.org/10.1111/jvim.15802.

29. A. J. Parker and R. D. Park, "Unusual Deformity of the Occipital Bone in a Dog (a Case Report)," *Veterinary Medicine and Small Animal Clinician* 69, no. 4 (1974): 438.

30. A. G. Watson, A. De Lahunta, and H. E. Evans, "Dorsal Notch of Foramen Magnum due to Incomplete Ossification of Supraoccipital Bone in Dogs," *Journal of Small Animal Practice* 30, no. 12 (1989): 666–673, https://doi.org/10.1111/j.1748-5827.1989.tb01911.x.

31. C. Rusbridge, F. Stringer, and S. P. Knowler, "Clinical Application of Diagnostic Imaging of Chiari-Like Malformation and Syringomyelia," *Frontiers in Veterinary Science* 5 (2018): 280, https://doi.org/10.3389/fvets.2018.00280.

32. B. V. Ineichen, S. V. Okar, S. T. Proulx, B. Engelhardt, H. Lassmann, and D. S. Reich, "Perivascular Spaces and Their Role in Neuroinflammation," *Neuron* 110, no. 21 (2022): 3566–3581, https://doi.org/10.1016/j.neuron.2022.10.024.

33. S. Xu, E. K. Jordan, S. Brocke, et al., "Study of Relapsing Remitting Experimental Allergic Encephalomyelitis SJL Mouse Model Using MION-46L Enhanced In Vivo MRI: Early Histopathological Correlation," *Journal of Neuroscience Research* 52, no. 5 (1998): 549–558, https://doi.org/10.1002/(SICI)1097-4547(19980601)52:5<549::AID-JNR7>3.0.CO;2-C.

34. T. Flegel, D. Henke, I. C. Boettcher, et al., "Magnetic Resonance Imaging Findings in Histologically Confirmed Pug Dog Encephalitis," *Veterinary Radiology & Ultrasound* 49, no. 5 (2008): 419–424, https://doi.org/10.1111/j.1740-8261.2008.00400.x.

35. K. A. Greer, A. K. Wong, H. Liu, et al., "Necrotizing Meningoencephalitis of Pug Dogs Associates With Dog Leukocyte Antigen Class II and Resembles Acute Variant Forms of Multiple Sclerosis," *Tissue Antigens* 76, no. 2 (2010): 110–118, https://doi.org/10.1111/j.1399-0039.2010.01484.x.

36. D. R. Cordy and T. A. Holliday, "A Necrotizing Meningoencephalitis of Pug Dogs," *Veterinary Pathology* 26, no. 3 (1989): 191–194, https://doi.org/10.1177/030098588902600301.

37. R. J. Higgins, P. J. Dickinson, S. A. Kube, et al., "Necrotizing Meningoencephalitis in Five Chihuahua Dogs," *Veterinary Pathology* 45, no. 3 (2008): 336–346, https://doi.org/10.1354/vp.45-3-336.

38. I. Spitzbarth, H. C. Schenk, A. Tipold, and A. Beineke, "Immunohistochemical Characterization of Inflammatory and Glial Responses in a Case of Necrotizing Leucoencephalitis in a French Bulldog," *Journal of Comparative Pathology* 142, no. 2–3 (2010): 235–241, https://doi.org/10.1016/j.jcpa.2009.08.158.

39. K. Baiker, S. Hofmann, A. Fischer, et al., "Leigh-Like Subacute Necrotising Encephalopathy in Yorkshire Terriers: Neuropathological Characterisation, Respiratory Chain Activities and Mitochondrial DNA," *Acta Neuropathologica* 118, no. 5 (2009): 697–709, https://doi.org/10.1007/s00401-009-0548-6.

40. J. M. Ducote, K. E. Johnson, C. W. Dewey, et al., "Computed Tomography of Necrotizing Meningoencephalitis in 3 Yorkshire Terriers," *Veterinary Radiology & Ultrasound* 40, no. 6 (1999): 617–621, https://doi.org/10.1111/j.1740-8261.1999.tb00888.x.

41. M. Kuwamura, T. Adachi, J. Yamate, T. Kotani, F. Ohashi, and B. A. Summers, "Necrotising Encephalitis in the Yorkshire Terrier: A Case Report and Literature Review," *Journal of Small Animal Practice* 43, no. 10 (2002): 459–463, https://doi.org/10.1111/j.1748-5827.2002.tb00014.x.

42. D. Lotti, M. T. Capucchio, E. Gaidolfi, and M. Merlo, "Necrotizing Encephalitis in a Yorkshire Terrier: Clinical, Imaging, and Pathologic Findings," *Veterinary Radiology & Ultrasound* 40, no. 6 (1999): 622–626, https://doi.org/10.1111/j.1740-8261.1999.tb00889.x.

43. J. N. Nessler, A. Oevermann, M. Schawacht, et al., "Concomitant Necrotizing Encephalitis and Granulomatous Meningoencephalitis in Four Toy Breed Dogs," *Frontiers in Veterinary Science* 9 (2022): 957285, https://doi.org/10.3389/fvets.2022.957285.

44. N. Jeffery and N. Granger, "New Insights Into the Treatment of Meningoencephalomyelitis of Unknown Origin Since 2009: A Review of 671 Cases," *Frontiers in Veterinary Science* 10 (2023): 1114798, https://doi.org/10.3389/fvets.2023.1114798.

45. R. Gonçalves, T. W. Maddox, S. Phillipps, et al., "Development of a Reliable Clinical Assessment Tool for Meningoencephalitis in Dogs: The Neurodisability Scale," *Journal of Veterinary Internal Medicine* 37, no. 3 (2023): 1111–1118, https://doi.org/10.1111/jvim.16717.

46. N. Hayashi, Y. Watanabe, T. Masumoto, et al., "Utilization of Low-Field MR Scanners," *Magnetic Resonance in Medical Sciences* 3, no. 1 (2004): 27–38, https://doi.org/10.2463/mrms.3.27.

47. C. Brekenfeld, E. Foert, W. Hundt, et al., "Enhancement of Cerebral Diseases: How Much Contrast Agent Is Enough? Comparison of 0.1, 0.2, and 0.3 Mmol/Kg Gadoteridol at 0.2 T With 0.1 mmol/kg Gadoteridol at 1.5 T," *Investigative Radiology* 36, no. 5 (2001): 266–275, https://doi.org/10.1097/00004424-200105000-00004.

48. M. Konar and J. Lang, "Pros and Cons of Low-Field Magnetic Resonance Imaging in Veterinary Practice," *Veterinary Radiology & Ultrasound* 52, no. 1 Suppl 1 (2011): S5–S14, https://doi.org/10.1111/j.1740-8261.2010.01780.x.